

The Development of a Mouse Model of Ovarian Endosalpingiosis

Sarah K. Bristol-Gould, Christina G. Hutten, Charles Sturgis, Signe M. Kilen, Kelly E. Mayo, and Teresa K. Woodruff

Department of Neurobiology and Physiology (S.K.B.-G., T.K.W.), Department of Biochemistry, Molecular Biology and Cell Biology (K.E.M.), and Center for Reproductive Science (C.G.H., S.M.K., K.E.M., T.K.W.), Northwestern University, and Evanston Northwestern Hospital (C.S.), Evanston, Illinois 60208; and Department of Medicine (T.K.W.) Feinberg School of Medicine, Northwestern University, and Robert H. Lurie Comprehensive Cancer Center of Northwestern University (T.K.W.), Chicago, Illinois 60611

Pelvic pain is a common presenting ailment in women often linked to ovulation, endometriosis, early pregnancy, ovarian cancer, and cysts. Clear differential diagnosis for each condition caused by these varied etiologies is difficult and may slow the delivery of therapy that, in the case of ovarian cancer, could be fatal. Ovarian endosalpingiosis, a pelvic condition typified by the presence of cystic glandular structures lined by benign tubal/salpingeal epithelium, is also associated with pelvic pain in women. The exact cellular antecedents of these epithelial lined cystic structures are not known, nor is there a known link to ovarian cancer. A mouse model of ovarian endosalpingiosis has been developed by directing a dominant-

negative version of the TGF- β transcription factor, Smad2, to the ovary using the Müllerian-inhibiting substance promoter (MIS-Smad2-dn). Female mice develop an ovarian endosalpingeal phenotype as early as 3 months of age. Importantly, cysts continuous with the ovarian surface epithelial have been identified, indicating that these cyst cells may be derived from the highly plastic ovarian surface epithelial cell layer. A second transgenic mouse model that causes loss of activin action (inhibin α -subunit transgenic mice) develops similar cystic structures, supporting a TGF- β /activin/Smad2 dependence in the onset of this disease. (*Endocrinology* 146: 5228–5236, 2005)

ENDOSALPINGIOSIS is a histopathologically recognized and not infrequently encountered condition identified in extratubal pelvic tissues in both pre- and postmenopausal women (1). It may be associated with pelvic pain and is characterized by the presence of extrasalpingeal cystic spaces lined by cells that phenocopy a tubal-type epithelium. Human ovarian endosalpingiosis is most commonly diagnosed as an incidental finding when tissues are surgically resected for other reasons. Other generally involved sites where endosalpingiotic lesions are found include the uterine serosa, omentum, urinary bladder, bowel wall, and pelvic lymph nodes (1–4). Neither the origin nor the transformative potential of these ectopic cells are understood; however, in many cases of endosalpingiosis additional pelvic pathologies are present (5). Case reports have found endosalpingiosis to be associated with ovarian surface papillary tumors, adenocarcinoma of the fallopian tubes, and endometriosis (5–8). In short of an animal model of endosalpingiosis coupled with the inability to track its course and lack of clinical correlation, there has been limited progress in understanding the condition and its implications to the health of affected women.

One of the prevailing views of the onset of ovarian

cancer is the transformation of cells that comprise the surface epithelium into neoplastic cysts, possibly caused by the process of ovulation (9–12). The TGF- β superfamily of ligands, particularly TGF- β and activin, have been implicated in the regulation of ovulation; therefore, we targeted the signaling pathway used by these two ligands in developing a mouse model that might generate early stage ovarian surface epithelial (OSE)-derived neoplasms. TGF- β is known to be important in the regulation of the OSE, whereas activin functions in the control of wound repair and scar formation (13–16). Both ligands use Smad2 and Smad3 as common transcriptional coregulators; therefore, we directed a Smad2 dominant-negative (Smad2-dn) transgene to the ovary.

The development of animal models of complex disease, especially those that present in a sexually dimorphic manner, has progressed significantly in the past 2 yr. Mouse models of endometriosis and endometrioid ovarian cancer have been developed using targeted genetic deletion of the *Pten* and *K-ras* genes in the OSE (17). Advances have been made in BRCA1 and BRCA2 mouse models that phenocopy breast and ovarian cancer, and Smad7 up-regulation appears to be important to the TGF- β -resistant endometrial cancers (18, 19). Our model targeted the ovary to reduce the TGF- β /activin signal transduction pathway. These studies suggest that the origin of the endosalpingiotic lesions are from the Müllerian epithelium and provide additional evidence that this cell type has a variety of endpoints to which it develops based on the genetic background and the microenvironment in which the cell exists.

First Published Online September 1, 2005

Abbreviations: CL, Corpora lutea; FITC, fluorescein isothiocyanate; MIS, Müllerian-inhibiting substance; MOF, multioocytic follicles; OSE, ovarian surface epithelium; Smad2-dn, Smad2 dominant-negative.

Endocrinology is published monthly by The Endocrine Society (<http://www.endo-society.org>), the foremost professional society serving the endocrine community.

Materials and Methods

Generation of transgenic animals

The genetic cassette used for creating the transgenic mice consists of a mouse minimal Müllerian-inhibiting substance (MIS) promoter (–180 bp), an epitope tag (Flag), a C-terminal truncation of the human Smad2

gene (dominant negative), and a human GH polyadenylation sequence (Fig. 1A). The DNA insert was digested free of vector sequence, purified by gel purification, and sent to the Northwestern University Transgenic and Targeted Mutagenesis Core Facility (CMIER) under the direction of Dr. Lynn Doglio, for pronuclear injection of one-cell stage mouse embryos on a CD-1 background. Injected embryos were reimplanted into

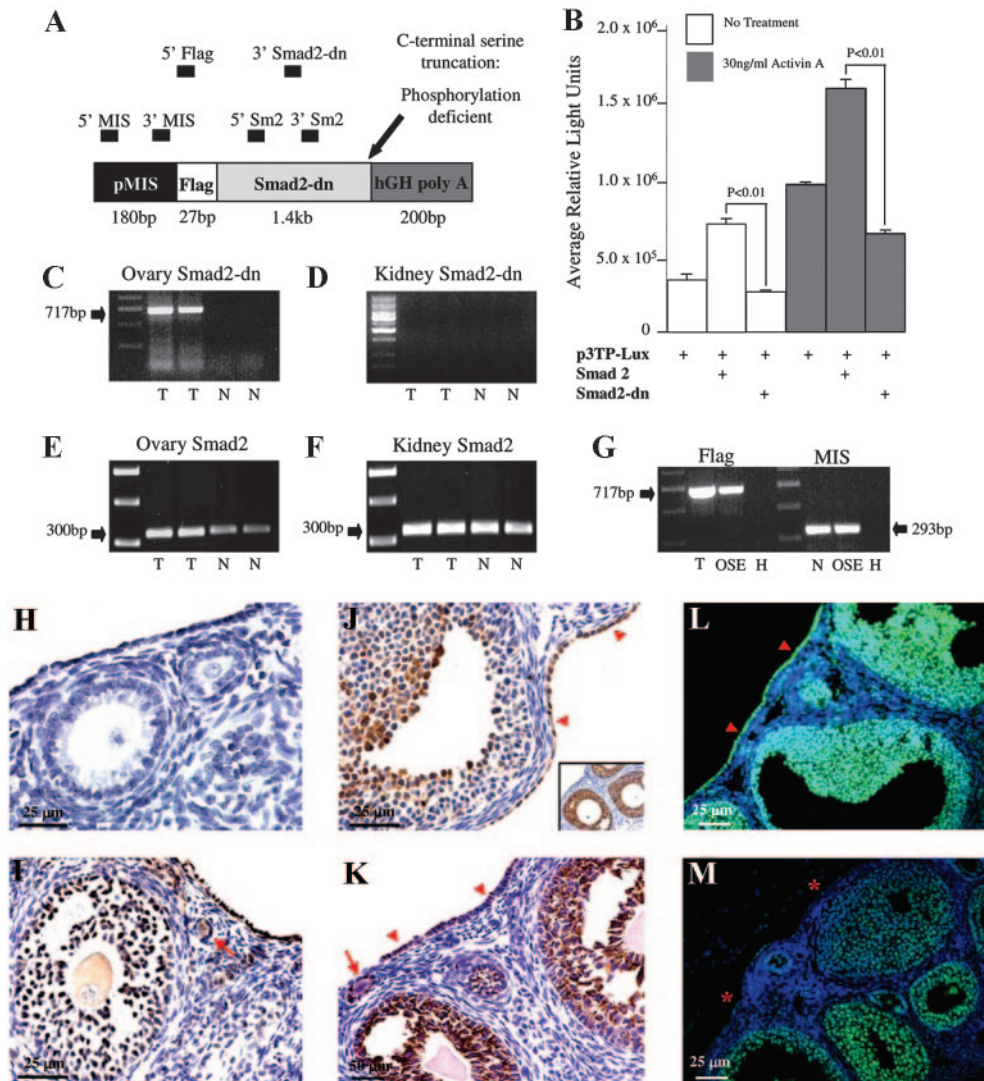


FIG. 1. Transgene construct actions *in vitro* and *in vivo*. **A**, The transgene construct includes a 180-bp promoter region of the mouse MIS gene fused to a C-terminally truncated human Smad2 protein by the flag epitope tag. The series of primers used for RT-PCR analysis and genotyping are designated above the map. **B**, Transfection of Smad2-dn into Cos-7 cells indicates that this protein induces a dominant-negative effect in cells at basal levels and in the presence of activin. Shown are mean values from three separate experiments \pm SEM. Statistical analysis was performed using a *t* test with variance indicated by SEM ($P < 0.01$). **C–G**, Expression of Smad2-dn transgene mRNA in mouse tissues. Whole ovary, kidney fragment, and isolated ovarian OSE RNA from transgenic (T) and normal littermate (N) mice were subjected to RT-PCR methods described in *Materials and Methods*. **C**, A 717-bp product shown in the T lanes indicates the presence of the transgene in transgenic ovaries, but not in normal littermate ovaries (N). **D**, The transgene is also not expressed in transgenic (T) or normal littermate (N) kidneys. **E** and **F**, A 300-bp product using primers for normal Smad2 shows expression in ovaries and kidneys regardless of genotype. **G**, Amplified Flag cDNA in transgenic ovaries (T) and in isolated transgenic OSE cells (OSE). Water controls run throughout the PCR process are indicated with an (H). **H–M**, Transgene localization in ovarian tissue. **H**, Normal littermate ovary depicting no production of flag protein in the follicles or the OSE. **I**, Transgenic ovary indicating flag protein immunolocalization in granulosa cells of a secondary follicle, a B/C primordial follicle (red arrow), and in the OSE. **J**, MIS protein located in granulosa cells of a small antral follicle and the OSE (red arrowheads) in normal littermate mice. The inset shows additional MIS protein production in the preantral follicle population. **K**, MIS located in the OSE (red arrowheads) and follicles of transgenic mice. B/C primordial follicle is indicated by the red arrow. **L–M**, Overlay images of phosphorylated Smad2 indicated by FITC, and nuclear stain indicated by 4',6-diamidino-2-phenylindole. **L**, Normal littermate ovary indicating strong phospho-Smad2 protein production in follicles, and high levels in the OSE (red arrowheads). **M**, Transgenic ovary depicting decreased phospho-Smad2 protein in the ovarian follicles, and little phospho-Smad2 in the OSE (red asterisks). **H–J** were photographed at $\times 400$ magnification, **K–M** were photographed at $\times 200$ magnification using bright-field and fluorescence microscopy, respectively.

pseudo-pregnant females. Weanlings were tail cut for purification of genomic DNA. To establish founder mice, tail DNA was genotyped by PCR using primers (5' primer: ACCATGGACTACAAGGACGAC, 3' primer: ACTGATATATCCAGGAGGTGG) designed to amplify a 717-bp product between the Flag epitope tag and the Smad2-dn coding region. Amplification was carried out for 30 cycles at an annealing temp of 58 C.

Breeding of transgenic mice

Three founder male mice were identified and used to establish three separate transgenic lines. Mice were maintained in accordance to the policies of the Northwestern University's Animal Care and Use Committee. Mice were housed and bred in a controlled barrier facility within Northwestern University's Center of Comparative Medicine. Temperature, humidity, and photoperiod (12-h light, 12-h dark) were kept constant. Founder line 1 was fed a diet containing phytoestrogens (Harlan Teklad irradiated 7912). Founder lines 2 and 3 were fed a phytoestrogen-free diet (Harlan Teklad Global 2019 or Harlan Teklad Breeder diet 2919). Founder line 1 was studied for well over a year before the line was lost (unrelated to the transgene). Founder lines 2 and 3 were subsequently generated and offspring were studied for over 1 yr. Data are presented for all three lines.

Cell culture and transient transfections

Cos-7 cells were maintained on 10-cm plates in DMEM supplemented with 10% fetal bovine serum, 1% antibiotic, 3.7 g/liter sodium bicarbonate, and incubated in a humidified atmosphere of 5% CO₂ at 37 C. At about 80% confluency, cells were split 1:5 into 24-well plates and transiently transfected 24 h later with 250 ng of the reporter DNA (p3TP-luciferase) and 25 ng of various expression vectors per well using LipoFectamine Plus Reagent (Invitrogen, Carlsbad, CA). DNA was balanced using empty vectors where needed. Cells were treated for 24 h with serum-free media or serum-free media plus Activin A (30 ng/ml). Measurement of luciferase activity was conducted as previously reported (20). Data presented are averages from three separate experiments.

OSE isolation

Ovaries were removed from 10 adult transgenic mice, and isolation was performed using a previously described method (21). Briefly, ovaries were placed in a culture dish containing Hanks' balanced salt solution at 4 C, followed by incubation in 10 ml Hanks' balanced salt solution with 0.2% trypsin for 30 min at 37 C and 5% CO₂. The media containing the epithelial cells was transferred to 5 ml DMEM (supplemented with 4% FBS, 100 U/ml penicillin, 100 µg/ml streptomycin, 5 µg/ml insulin, 5 µg/ml transferrin, and 5 ng/ml sodium selenite) and pelleted by centrifugation. The pellet was resuspended in 2 ml of DMEM and placed in a single well of a six-well culture dish. Cells were cultured for 3 wk before RNA isolation.

RNA extraction and RT-PCR

Ovarian and kidney total RNA was extracted from transgenic and normal littermate mice using TRIZOL (Life Technologies Inc., Rockville, MD). Total RNA from the OSE cells was extracted using RNeasy Mini Kit (QIAGEN, Valencia, CA). Two to four micrograms were reverse transcribed into cDNA using Moloney murine leukemia virus reverse transcriptase in the presence of 20 pmol random hexamer oligonucleotides and 10 mM deoxynucleotide triphosphates (Promega Corp., Madison, WI). PCR was performed on transgenic and normal littermate ovarian and kidney cDNA for Smad2 using 35 cycles with annealing temperatures of 58 C, and Smad2-dn using 35 cycles with annealing temperatures of 52 C. For Smad2 a 300-bp product was expected using the following primers: 5' primer: CTCCAGTCTAGTGCCTCGG, 3' primer: AACACCAGAATGCAGGTTCC. For Smad2-dn, a 717-bp product was amplified using the same primers designed for genotyping. PCR was performed on transgenic OSE cell cDNA for MIS using 35 cycles with an annealing temperature of 58 C and also for Smad2-dn using 35 cycles with annealing temperatures of 58 C. For MIS, a 293-bp product was expected using the following primers: 5' primer: TTGCTGAAGT-

TCCAAGAGCCTCCA, 3' primer: GAAACAGCGGAATCAGAGC-CAAA.

Immunohistochemistry and antibodies

Immunohistochemistry was performed using a previously described method (22). For all instances, replacing the primary antibody with buffer and adding only secondary antibody was used as a negative control. Immunohistochemical images were acquired on a Nikon E600 microscope (Fryer Co. Inc., Huntley, IL) using a Spot Insight Mosaic 11.2 color digital camera and Advanced Spot Imaging software (version 4.6, Universal Imaging, Downingtown, PA). Immunofluorescent images were acquired on a Nikon E600 microscope using a Spot RT monochrome digital camera (Diagnostic Instruments) and Metamorph Imaging Software (version 4.9; Universal Imaging). The antigens stained by immunohistochemistry included flag, phospho-Smad2, MIS, cytokeratin 19 (CK-19) and cytokeratin 8 (CK-8). The primary antibodies used were chicken polyclonal antibody to flag (a gift from Dr. Larry Jameson, Feinberg School of Medicine, Chicago, IL), rabbit polyclonal antibody to phosphorylated Smad2 (Cell Signaling Technology, Inc., Beverly, MA), goat polyclonal antibody to MIS (Santa Cruz Biotechnology, Inc., Santa Cruz, CA), CK-19 (a gift from Dr. Barbara Vanderhyden, University of Ottawa, Ottawa, Canada), and rat monoclonal antibody TROMA 1 to CK8 (Developmental Studies Hybridoma Bank, The University of Iowa, Iowa City, IA). Dilutions of the primary antibodies for flag, phospho-Smad2, MIS, CK-19 and CK-8 were 1:100, 1:50, 1:200, 1:100, and 1:50, respectively.

Fertility measurements

Transgenic and control female mice were paired with proven breeder CD-1 male mice. Each mating pair was housed together for an average of 7 months. The pairs were set up once breeding age was reached (~65 d). The litter sizes of each mating pair were averaged at the time of birth, and the time interval between births was recorded as number of litters per month.

Hormone measurements

Serum FSH was measured by RIA (Ligand Assay and Analysis Core Laboratory, Center for Research in Reproduction, University of Virginia, Charlottesville, VA). The FSH RIA had a detection range of 3.5–30.7 ng/ml. The average intraassay and interassay coefficients of variation are from 4.6–14.4%, respectively.

Results

Structure of transgene and function *in vitro*

The Smad2-dn transgene was targeted to the gonads in transgenic mice using a minimal mouse MIS promoter that has been reported to direct transgene expression to testicular Sertoli cells and ovarian granulosa cells (Fig. 1A). The transgene construct generated includes the coding regions of human Smad2 but lacks three C-terminal serine residues that are normally phosphorylated as a consequence of TGF- β or activin receptor activation (23). The C terminus is required for Smad2 biological activity; therefore, this truncation renders the protein capable of docking to a receptor but unable to act as a substrate and initiate downstream signal transduction events (24, 25). Many laboratories including our own have used this transgene to decrease activin signaling *in vitro* (23). To test the transgene activity *in vitro*, cos-7 cells were transfected with p3TP-luciferase, a known promoter target for activated Smads, in addition to Smad2 and Smad2-dn constructs (Fig. 1B). In the presence of activin the luciferase response level increases with Smad2 transfection, and decreases significantly with Smad2-dn transfection. The Smad2-dn construct demonstrates a true dominant-negative

effect in these cells at basal levels and in the presence of activin.

Transgene expression in vivo

The tissue distribution of the transgene was examined using specific primers and RT-PCR amplification of RNA isolated from whole ovary and kidney fragments of transgenic and normal littermate animals in addition to the OSE cells of transgenic ovaries (Fig. 1, C–G). The transgene (717-bp product) was expressed in transgenic ovaries but not in transgenic mouse kidneys, nor in either tissue isolated from normal littermates (Fig. 1, C–D). The endogenous mouse Smad2 gene (300-bp product), was detected in all tissues regardless of genotype (Fig. 1, E and F). To verify cell-specific expression, the transgene (Flag-Smad2-dn) and MIS were also amplified from transgenic OSE cell RNA (Fig. 1G). We further analyzed the chimeric flag-Smad2-dn protein by immunolocalization in ovaries of both genotypes. The flag epitope was not detected in any cell types within normal littermate mouse ovarian tissue (Fig. 1H). Flag protein was detected in ovarian follicles of transgenic mice as early as the B/C primordial follicle (transitory primordial follicle containing squamous and cuboidal granulosa cells) stage, in addition to being localized within portions of OSE (Fig. 1I). MIS protein was detected in granulosa cells of preantral and small antral follicles in mice of both genotypes. MIS was also detected in portions of the OSE in normal littermate and transgenic ovaries (Fig. 1, J and K). Because the transgene was expected to block endogenous Smad2 activity, the presence and cellular location of phosphorylated Smad2 was immunolocalized to cells within the ovaries. Nuclear Smad2 was detected in the granulosa cells of all follicles regardless of genotype; however, levels were slightly decreased in nearly half the transgenic ovaries analyzed [decreased fluorescein isothiocyanate (FITC) stain in granulosa cells in Fig. 1M]. Conversely, phospho-Smad2 was not detected in the majority of OSE cells in transgenic mice, whereas normal littermate animals had robust levels of nuclear Smad2 in the OSE (Fig. 1, L and M). We quantified the amount of fluorescence in these panels by counting positively (FITC labeled) stained OSE cells. In the transgenic animals, 28% of OSE cells stained for phosphorylated Smad2, whereas 79% of OSE cells stained for phosphorylated Smad2 protein in normal littermate mice. Together, these RNA and protein data suggest that our transgene is targeted to the ovarian granulosa cells and the OSE but may have the most impact on the OSE cell population based on subsequent observations.

Fertility studies and serum FSH levels

Smad2-dn female mice were subfertile with a decreased litter size and breeding frequency in comparison to control breeding animals. Control CD-1 breeding mice had an average pup number at birth of 16.9, and a breeding frequency of 1.2 litters per month ($n = 3$). The transgenic breeding mice had an average pup number at birth of 11.0, and a breeding frequency of 1.0 litter per month ($n = 6$). In two of six transgenic breeder females, there was a delay in first pregnancy by 2 months of setting up the mating pairs (the other four breeders became pregnant shortly after the males were

introduced), followed by a complete cessation of breeding after only two gestations. Considering the transgene is expressed in the granulosa cells of developing follicles, there might be an affect to normal folliculogenesis in our transgenic animals that subsequently alters fertility. Quantification of follicle populations and possible differences are ongoing. Endosalpingiosis does not normally present as a disease that causes infertility. However, because the condition is often incidentally found and because there is no diagnosis of the syndrome, it is not yet known whether there is a direct link between the fertility issues in our mice and the eventual development of endosalpingiosis.

There were fewer corpora lutea (CL) in Smad2-dn transgenic mouse ovaries compared with ovaries from normal littermates. When CL were counted in serial sectioned ovaries from animals ranging in age from 5–6 months, the average number present in normal littermate animals was significantly higher ($P < 0.003$) than that present in transgenic animals. Normal littermate mice had an average of 23.6 CL ($n = 3$), whereas transgenic animals had an average of 16.4 CL ($n = 4$). Additionally, serum FSH levels were measured and no significant difference between 3-month-old transgenic and normal littermate mice was found (data not shown). Therefore, suggesting that our transgene is only having a local ovarian affect.

Ovarian pathologies I: stroma, crypts, and invaginations

As the ovary ages it becomes increasing irregular in shape. However, many of the ovarian phenotypes that are commonly associated with middle and old age begin to appear in our transgenic animals by 3 months of age, and continually worsen. Stromal disorganization (classified as a stroma occupied with holes instead of densely packed with follicles and CL) was apparent in the medullary regions in most transgenic ovaries at all ages examined. Cryptic structures and epithelial invaginations began to emerge anywhere from 3–5 months in our animals. Crypts tend to be located near the hilus, whereas the invaginations resided near the outside edge of the ovary and invaginate inwards. The cells lining the crypts and invaginations display many characteristics of epithelial cells: columnar shape, basally oriented nucleus, and ciliation (Fig. 2, A and B). These cells may originate from the ovarian surface epithelium or they may come from the epithelial cells that line the rete ovarii.

Ovarian pathologies II: lesions, inclusions, and cysts

During postovulatory repair in the mouse and human, it is commonly thought that displaced OSE cells either revert to an epithelial cell phenotype or go through an epithelial to mesenchymal transition. If incomplete transition takes place, cells can be incorporated into the stroma near the site of ovulation and likely form inclusion cysts (10). Different types and conformations of serous, benign, cystic structures/lesions were commonly found in Smad2-dn mice around 8–12 months of age, but we have also identified cyst formation as early as 3 months (Fig. 3). Most transgenic ovaries contained multiple small lesions/inclusion cysts representative of classic ovarian endosalpingiosis seen in humans. Whereas other transgenic ovaries possessed one large cyst that was either

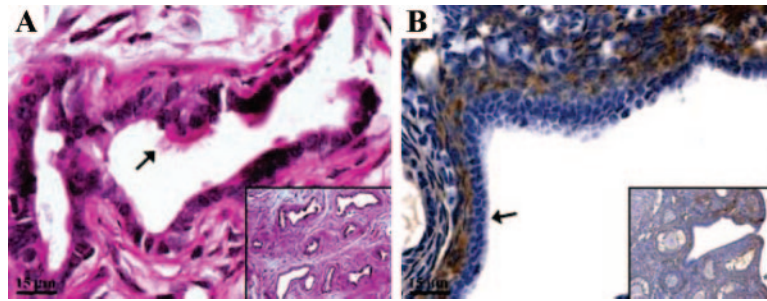


FIG. 2. Ovarian crypts and invaginations in transgenic mouse ovaries. A, Crypt-like structures found throughout the ovarian stroma (usually near the hilus) in many transgenic mouse ovaries. Cells are cuboidal in shape, have a basally oriented nucleus, and contain cilia (*black arrow*). *Inset* is a $\times 200$ magnification of A that was photographed at $\times 600$ magnification. B, Invaginations of the ovarian surface frequently seen in young transgenic animals photographed at $\times 600$ magnification. Cells are cuboidal in shape, ciliated (*black arrow*), and tend to layer upon each other in certain areas. *Inset* is a $\times 200$ magnified image of where these invaginations are usually found. *Black asterisks* mark the edge of the ovary.

fluid filled (in resemblance to those found in the inhibin- α transgenic mice) or contained a mass of cells, the origin of which is not known (Fig. 3, D–F). Although cyst types were different in gross appearance, microscopic evaluation, number and location, the cells that line the cysts were epithelial in origin based on histomorphology.

The single layer of epithelium lining all the cysts is similar to a tubal-type epithelium. Three basic cell types are present

in various numbers that resemble the three cell types found in the normal fallopian tube in women (oviduct in the mouse): pale focally ciliated cells, secretory or vacuolated cells, and dark intercalated cells with prominent basal nuclei (Fig. 4). The cysts often exhibit irregular contours and occasional intraluminal stromal papillae. All of these characteristics associate with an endosalpingiosis phenotype more so than a serous cystadenoma phenotype.

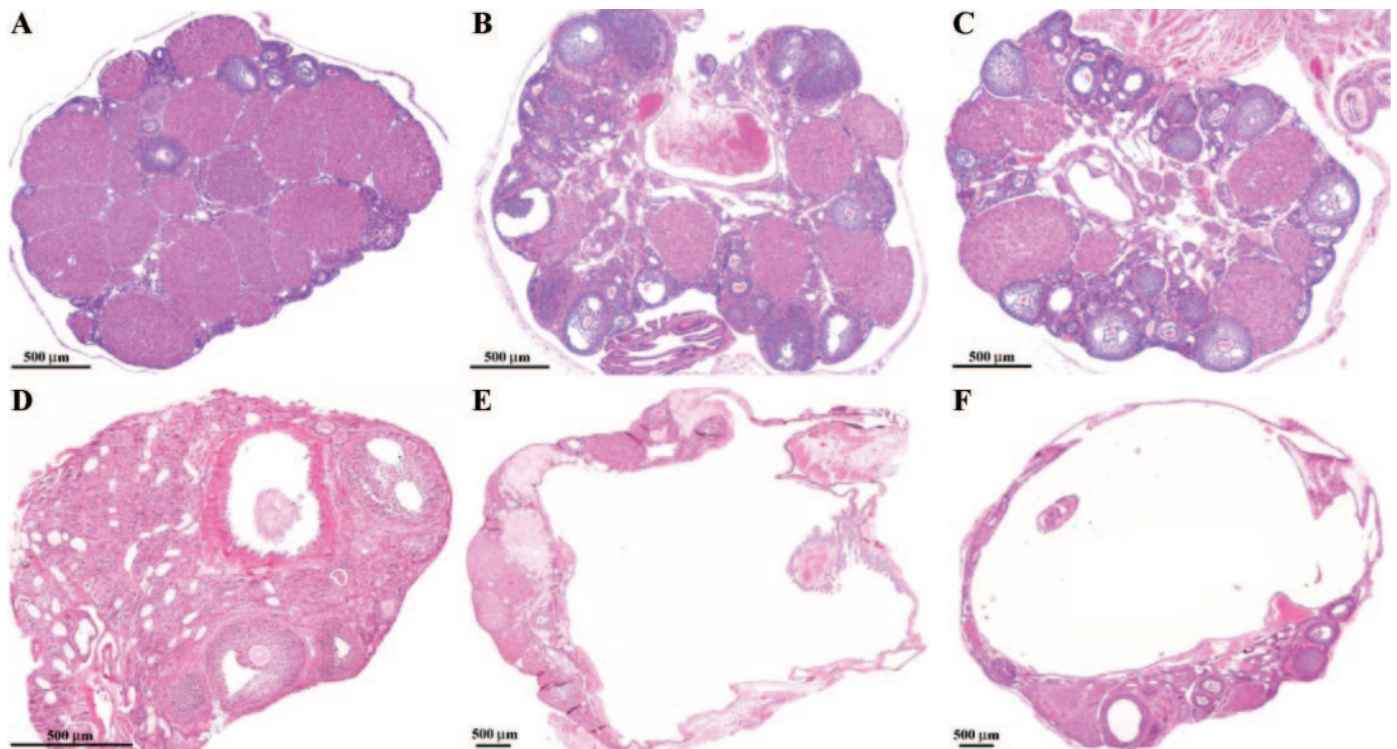


FIG. 3. Ovarian histology of transgenic mice. Ovaries were fixed in 4% paraformaldehyde, embedded in paraffin, sectioned, and stained with hematoxylin and eosin only. Detection of cysts begins at 3.5 months and ranges in age to 11 months old. A, 5- μ m section of an ovary from a 5-month-old normal littermate mouse showing normal histology. B, A 5- μ m section of an ovary from a 3.5-month-old transgenic mouse showing a large cyst near the hilus of the ovary, continuous with the OSE, and filled with cells. C, A 5- μ m section of an ovary from a 5-month-old transgenic mouse showing a more centrally located cyst. This image is taken in the beginning of the cyst, subsequent serial sections show the cyst increasing dramatically in size and stretching all the way to the edge of the ovary. D, A 5- μ m section of an ovary from a 9-month-old transgenic mouse showing a developed cyst containing a cellular mass within. This cyst is located in the outer portion of the ovary (this section is not cut through the center of the ovary). E, A 5- μ m section of an ovary from a 9-month-old transgenic mouse representing the largest type of cyst found. F, A 5- μ m section of an ovary from an 11-month-old transgenic mouse with another very large fluid filled cyst. These fluid filled cysts are very similar to those seen in the inhibin- α subunit transgenic mice. All images were photographed at $\times 100$ magnification.

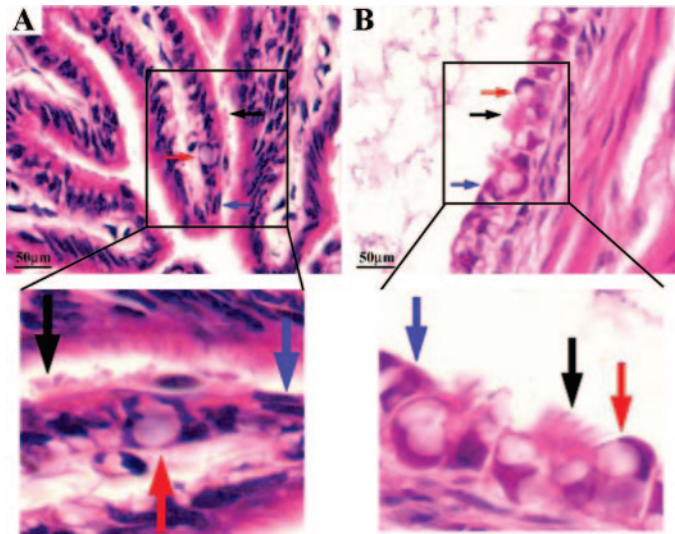


FIG. 4. Comparison of cells lining the cysts *vs.* cells lining the oviduct. A, $\times 1000$ Magnification of cells within the oviduct. B, $\times 1000$ Magnification of cyst cellular lining in a transgenic ovary. Below panels A and B are enlarged representations of areas containing the three types of cells of interest. *Black arrows* indicate ciliated cells, *red arrows* indicate secretory cells, and *blue arrows* indicate intercalated or peg cells.

To distinguish and verify the cell type lining the cysts, we stained sections for epithelial cell markers CK-19 and CK-8, and a granulosa cell marker inhibin α -subunit. CK-19 was detected in those cells that line the cysts and in OSE cells; however, CK-19 was not detected in the granulosa cells of follicles (Fig. 5, B and B'). As expected, the inhibin α -subunit protein was detected in the granulosa cells of follicles but was not detected in the cells lining the cyst, confirming that the cyst cells are not granulosa cells (Fig. 5, C and C'). CK-8 was also detected in cells lining cysts formed in *Smad2-dn* ovaries and was not detected in follicular granulosa cells confirming the CK-19 results (Fig. 5, E and E'). Furthermore, CK-8 protein was detected in the OSE (Fig. 5F).

A second animal model generated to block the activin signal transduction system is the inhibin α -subunit transgenic mouse (26). Importantly, the inhibin α -subunit transgene is driven by a metallothionein-I promoter and is therefore ubiquitously expressed. However, similar to the *Smad2-dn* mice, the inhibin α -subunit transgenic females are subfertile and develop ovarian cysts (26). The cysts are also lined by tubal-type cells that stain positively for CK-8, whereas the granulosa cells fail to stain with this marker (Fig. 5, H and I).

Ovarian phenotype III: multioocytic follicles (MOFs)

The final phenotype encountered in both the *Smad2-dn* and the inhibin α -subunit transgenic mice is the formation of MOFs (26). Although present at a low frequency, several types of MOFs appeared in founder line 1 transgenic animals. The most commonly detected MOFs were two oocytes per follicle. MOFs in the *Smad2-dn* mice appear in two configurations based on the encapsulated oocytes. Oocytes of some MOFs may possibly retain their embryonic connections (Fig. 6B). Although more commonly, MOFs were detected that

have independent separated oocytes (Fig. 6, C and D). The somatic cells in the latter type of MOF have completely surrounded each individual oocyte, but a basement membrane has not. Interestingly, MOFs were not detected in *Smad2-dn* founder lines 2 and 3 kept on the phytoestrogen-free diet; however, when these transgenic animals were switched back to the original phytoestrogen-containing food, the MOFs reappeared in these lines (data not shown).

Discussion

Endosalpingiosis can be diagnosed, but its onset, progression, and implications for risk of other health complications is not completely understood. Two animal models that converge on the TGF- β /activin signal transduction pathway and develop this condition can now be studied to provide answers to these important questions. The histogenesis of endosalpingiosis is debatable because the origins of the cells lining the cysts are not known for certain. The first prospect is that the cells are ovarian surface epithelia. The surface epithelium of the ovary is a single, simple epithelial layer of cells that undergoes dramatic reorganization during each ovulatory cycle. By unknown mechanisms, the OSE may become trapped within the stroma and instead of assuming a mesenchymal phenotype these cells undergo metaplasia to become Müllerian-like epithelia (27). These tubal-type epithelia may therefore make up the lining of the inclusion cysts that are often assumed to be the precursors of neoplastic progression (27, 28).

The OSE and extraovarian mesothelium are both derived embryonically from the celomic epithelium and exist in a similar environment. However, in the adult, the two differentiated cell populations express the epithelial differentiation marker CA125 (also the tumor marker for ovarian and Müllerian duct-derived neoplasms) differently (29). CA125 is expressed in adult oviductal, endometrial, and endocervical epithelia, but not the OSE (10, 30). The OSE is a fairly undifferentiated cell and it is thought that the accumulation of mutations in specific genes during ovulation can cause the OSE to differentiate into the serous, mucinous, or endometrial lineages associated with ovarian cancer. These varied cell fates suggest that the adult OSE may not be fully differentiated and that it possesses an intrinsic plasticity or pleuripotential resembling its mesodermal embryonic precursor more than the other celomic epithelial derivatives (oviduct, endometrium, cervix) (10). Given that the OSE never acquired CA125 or lost it early in development, unlike the other celomic derivatives, suggests that this cell layer might be less committed to a particular phenotype in the adult. OSE transformation or differentiation probably also depends on the genetic and, very likely, the hormonal milieu.

The cell origin discrepancy arises due to the fact that the common subtypes of ovarian cancer (serous, mucinous, and endometrioid) resemble epithelia that are not ovarian-like and are not normally present in the ovary itself (31). Hence, the second potential origin of cells lining the endosalpingiotic cysts may be structures that are embryologically derived from the Müllerian ducts themselves (oviduct, uterus, endometrium, rete ovarii) as opposed to the OSE. Considering the serous appearance of our cysts, it is a formal possibility

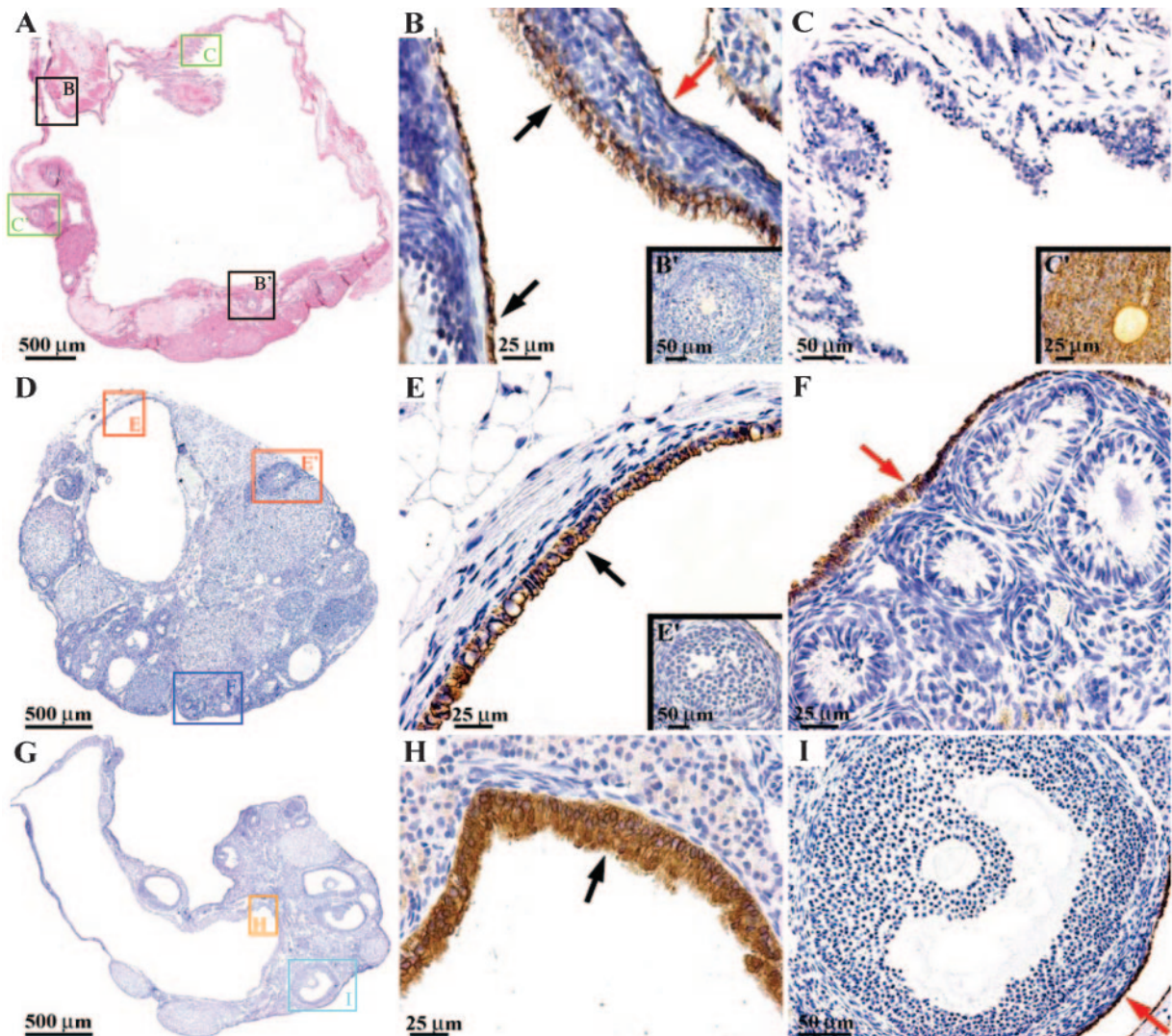


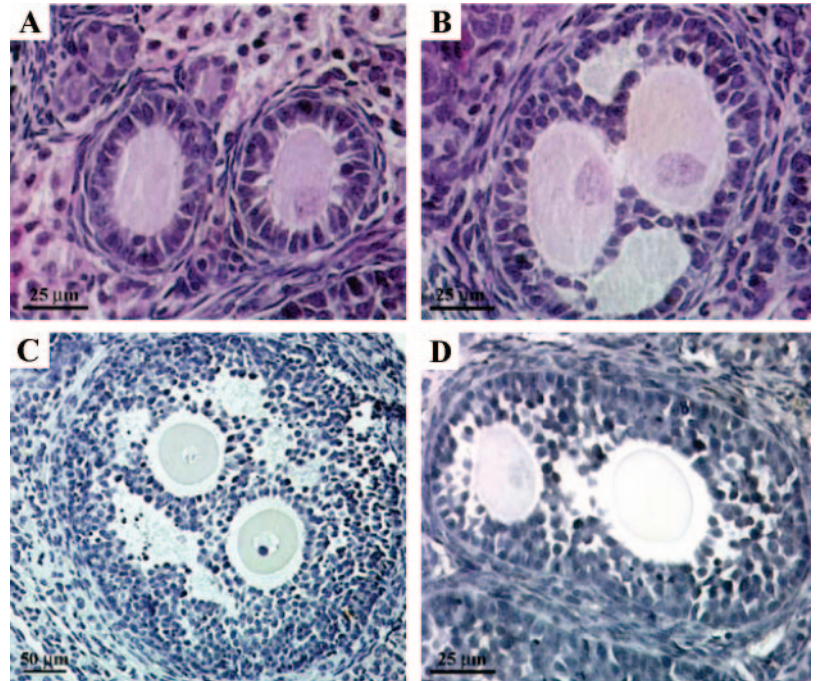
FIG. 5. Immunohistochemistry on cells lining the cysts in *Smad2-dn* and inhibin α -subunit transgenic ovaries. A, D, and G, $\times 100$ Magnification of transgenic ovaries containing large cysts. Boxes indicate positions that subsequent panels focus in on for immunohistochemical analysis. B, CK-19 staining in cells lining the cyst (black arrows) and the OSE (red arrow) taken at $\times 400$ magnification. B', Granulosa cells of follicles do not stain positive for CK-19, image taken at $\times 200$ magnification. C, $\times 200$ Magnification of cells lining the cyst that do not stain positive for inhibin α protein. C', $\times 400$ Magnification of granulosa cells in follicles that do produce high levels of inhibin α protein. E, CK-8 staining in cells lining the cyst (black arrow), image taken at $\times 400$ magnification. E', Granulosa cells of follicles do not stain positive for CK-8, image taken at $\times 200$ magnification. F, $\times 400$ Magnification of OSE cells that stain positive for CK-8 protein. H, $\times 400$ Magnification of cells lining a cyst in the inhibin α -subunit transgenic mice that do produce high amounts of CK-8 protein (black arrow). I, CK-8 staining is not present in granulosa cells of follicles, but is present in the OSE cells (red arrow) in inhibin α -subunit transgenic mice, image taken at $\times 200$ magnification.

that components of the secondary Müllerian system contribute these cells. This is possible if there is a developmental change in the expansion or differentiation of the celomic epithelium during development leading to embryologic rests of the Müllerian-type tissue. Dubeau (31) suggests that a portion of the secondary Müllerian system may not develop fully leaving remnants that may only differentiate under pathological conditions. If a second hit, such as loss of TGF- β signaling occurs, these cells may differentiate into the cystic structures that develop in our two mouse models. A fate map for these cells can now be examined with the two animal models created in our laboratories.

TGF- β and activin are involved in cell fate decisions and, in this case, may maintain the epithelial cell morphology

associated with cells on the ovarian surface. TGF- β is important to cell cycle control, whereas activin is implicated in wound healing, providing two mechanisms by which the agonists of this signaling pathway might be involved in maintaining the normal OSE (32, 33). The loss of this regulation in the *Smad2-dn* and inhibin α -subunit transgenic mouse models may result in the transition of some OSE into this tubal-type, more Müllerian-like morphology and result in cysts lined with these epithelia. Whether another alteration (such as the loss of p53 associated with ovulation) or other insults to the cell will create the next step in oncogenesis is not known. It is widely held that endosalpingiosis is a benign condition; however, it may be impacted by tamoxifen treatment indicating that the cells can be influenced by steroid

FIG. 6. MOF phenotype. Hematoxylin and eosin-stained sections of normal littermate and transgenic mouse ovaries. **A**, Two adjacent individual primary follicles in a normal littermate mouse ovary. **B**, Smad2-dn MOF that appears to retain oocyte connections and/or contains a granulosa cell invasion defect. **C** and **D**, MOFs possibly formed by a different mechanism than that seen in **B**. The oocytes here are completely surrounded by granulosa cells. Sections were photographed at $\times 400$ magnification, except **C**, which is $\times 200$ magnified using bright-field microscopy.



background (34). A link between endosalpingiosis and ovarian cancer or other gynecological cancers has not been established but warrants further investigation.

Chodankar *et al.* (35) used the Cre-lox system to inactivate BRCA1 in granulosa cells by using the FSH receptor promoter as the driver. However, the inactivation of the BRCA1 gene in the granulosa cells surprisingly led to the development of cystic structures lined by cells of epithelial morphology, not granulosa cells. They hypothesize that the granulosa cells act at a distance to control Müllerian epithelial tumorigenesis via a mechanism regulated by BRCA1. Signaling between granulosa cells and the OSE must occur given the requirement of ovulation at an explicit site on the ovarian surface. Because the transgene in our mice is expressed in both granulosa and OSE cells, we are unable to rule out the potential of defective signaling from the granulosa cells contributing to the cyst phenotype we observe. It is possible to speculate that the transgene directly functions in the granulosa cell population that then indirectly impacts the OSE or rete ovarii at a distance. How pathologies of the OSE are influenced by the granulosa cell compartment is an intriguing area of future investigation.

In general, the ovaries of the young transgenic mice seem to develop morphologies we would commonly associate with old age. The irregular shape, crypts, invaginations, inclusions, and cysts have historically been observed in wild-type mice close to 1 yr of age. Therefore, the ovarian age does not match the chronological age of the mouse. This is true of many idiopathic infertility patients, women who enter menopause early in reproductive life, and many PCOS patients (36–39). In each of these cases, the women are said to have ovaries that are older than their chronological age. An exception to this is a study which found PCOS patients entered menopause at older ages than normal women therefore suggesting these women's ovarian age to be younger than chronological age (40).

The two mouse models share a second phenotype, the development of MOFs. A mechanism by which individual follicles become encapsulated by granulosa cells has not been determined; however, it is likely that estrogen plays an important role in the process and notably there may be significant cross talk. We are currently investigating the effect of phytoestrogen containing food on the formation of these structures as this could be a confounding factor in whether or not MOFs form in our transgenic founder mice lines. Overall, the inappropriate encapsulation of follicles in the Smad2-dn and inhibin α -subunit transgenic mouse models suggests that the TGF- β /activin signal transduction pathway may somehow be involved. Neonatal exposure to estrogens results in an increased incidence of MOFs, which suggests a link between the steroid hormone and peptide hormone control of follicle development (41). We hypothesize that MOFs form through the absence of an imposed signal to identify the outside border of the follicle thus resulting in groups of oocytes retaining intracellular connections formed during development that subsequently are not broken throughout germ line cyst breakdown. The basement membrane and somatic cells that usually encapsulate one oocyte per follicle somehow are misregulated and do not form the normal follicle borders. It is also unknown whether the MOFs we detect ovulate. If so, they potentially cause more damage to the ovarian surface epithelium, and therefore could increase the probability of cyst formation in adult life.

Generation of animal models for gender-specific diseases are crucial in revealing important new mechanisms by which genes work in a male or female environment. Males from the Smad2-dn and inhibin α -subunit transgenic backgrounds do not have any known phenotypes that directly impact fertility. Therefore, the ability to manipulate specific cellular functions in a sexually dimorphic manner provides insight into the hormonal and genetic requirements for cellular function. The origins of many diseases of the female reproductive tract

are unknown and consequently difficult to treat. Pelvic pain is a frequent symptom with multiple etiologies. Therefore, it is necessary to continue to develop new diagnostics and expand treatment options to better understand the endosalpingiosis condition and intervene to improve the lives of women.

Acknowledgments

We would like to thank the Northwestern University Transgenic and Targeted Mutagenesis Core Facility (CMIER) for creating our founder transgenic lines. Andrew Lisowski in the P01 core facility for sectioning all tissue analyzed in this study. Jessica Kroger for her initial analysis of the Smad2-dn ovarian tissue. Dr. Joanna Burdette for her assistance with the OSE isolation protocol and overall experimental advice.

Received June 10, 2005. Accepted August 25, 2005.

Address all correspondence and requests for reprints to: Teresa K. Woodruff, Ph.D., Professor, Northwestern University, Department of Neurobiology, O. T. Hogan 4-150, 2205 Tech Drive, Evanston, Illinois 60208. E-mail: tkw@northwestern.edu.

This work was supported by Core services of University of Virginia Center for Research in Reproduction Ligand Assay and Analysis Core National Institute of Child Health and Human Development (NICHD) (Specialized Cooperative Centers Program in Reproduction Research) Grant U54-HD28934. National Institutes of Health (NIH)/NICHD Hormone Signals that Regulate Ovarian Differentiation, P01 HD021921. S.K.B.-G. received funding from the NIH/National Cancer Institute Training Program in Oncogenesis and Development Biology, T32 CA080621.

References

- Clement PB, Seidman JD, Russell P, Kurman RJ 2002 Blaustein's pathology of the female genital tract. 5th ed. New York: Springer
- Zinsser KR, Wheeler JE 1982 Endosalpingiosis in the omentum: a study of autopsy and surgical material. *Am J Surg Pathol* 6:109–117
- McCaughy WT, Schryer MJ, Lin XS, Al-Jabi M 1986 Extraovarian pelvic serous tumor with marked calcification. *Arch Pathol Lab Med* 110:78–80
- Sneig N, Fernandez T, Copeland LJ, Katz RL 1986 Mullerian inclusions in peritoneal washings. Potential source of error in cytologic diagnosis. *Acta Cytol* 30:271–276
- Heinig J, Gottschalk I, Cirkel U, Diallo R 2002 Endosalpingiosis—an underestimated cause of chronic pelvic pain or an accidental finding? A retrospective study of 16 cases. *Eur J Obstet Gynecol Reprod Biol* 103:75–78
- Ryuko K, Miura H, Abu-Musa A, Iwanari O, Kitao M 1992 Endosalpingiosis in association with ovarian surface papillary tumor of borderline malignancy. *Gynecol Oncol* 46:107–110
- Yeung HH, Bannatyne P, Russell P 1983 Adenocarcinoma of the fallopian tubes: a clinicopathological study of eight cases. *Pathology* 15:279–286
- deHoop TA, Mira J, Thomas MA 1997 Endosalpingiosis and chronic pelvic pain. *J Reprod Med* 42:613–616
- Fathalla MF 1971 Incessant ovulation—a factor in ovarian neoplasia? *Lancet* 2:163
- Auersperg N, Wong AS, Choi KC, Kang SK, Leung PC 2001 Ovarian surface epithelium: biology, endocrinology, and pathology. *Endocr Rev* 22:255–288
- Scully RE 1995 Pathology of ovarian cancer precursors. *J Cell Biochem Suppl* 23:208–218
- Tan OL, Hurst PR, Fleming JS 2005 Location of inclusion cysts in mouse ovaries in relation to age, pregnancy, and total ovulation number: implications for ovarian cancer? *J Pathol* 205:483–490
- Berchuck A, Rodriguez G, Olt G, Whitaker R, Boente MP, Arrick BA, Clarke-Pearson DL, Bast Jr RC 1992 Regulation of growth of normal ovarian epithelial cells and ovarian cancer cell lines by transforming growth factor- β . *Am J Obstet Gynecol* 166:676–684
- Nilsson EE, Skinner MK 2002 Role of transforming growth factor beta in ovarian surface epithelium biology and ovarian cancer. *Reprod Biomed Online* 5:254–258
- Munz B, Smola H, Engelhardt F, Bleuel K, Brauchle M, Lein I, Evans LW, Huylebroeck D, Balling R, Werner S 1999 Overexpression of activin A in the skin of transgenic mice reveals new activities of activin in epidermal morphogenesis, dermal fibrosis and wound repair. *EMBO J* 18:5205–5215
- Wankell M, Munz B, Hubner G, Hans W, Wolf E, Goppelt A, Werner S 2001 Impaired wound healing in transgenic mice overexpressing the activin antagonist follistatin in the epidermis. *EMBO J* 20:5361–5372
- Dinulescu DM, Ince TA, Quade BJ, Shafer SA, Crowley D, Jacks T 2005 Role of K-ras and Pten in the development of mouse models of endometriosis and endometrioid ovarian cancer. *Nat Med* 11:63–70
- Moynahan ME 2002 The cancer connection: BRCA1 and BRCA2 tumor suppression in mice and humans. *Oncogene* 21:8994–9007
- Dowdy SC, Mariani A, Reinholz MM, Keeney GL, Spelsberg TC, Podratz KC, Janknecht R 2005 Overexpression of the TGF- β antagonist Smad7 in endometrial cancer. *Gynecol Oncol* 96:368–373
- Suszko MI, Lo DJ, Suh H, Camper SA, Woodruff TK 2003 Regulation of the rat follicle-stimulating hormone β -subunit promoter by activin. *Mol Endocrinol* 17:318–332
- Roby KF, Taylor CC, Sweetwood JP, Cheng Y, Pace JL, Tawfik O, Persons DL, Smith PG, Terranova PF 2000 Development of a syngeneic mouse model for events related to ovarian cancer. *Carcinogenesis* 21:585–591
- Bristol SK, Woodruff TK 2004 Follicle-restricted compartmentalization of transforming growth factor β superfamily ligands in the feline ovary. *Biol Reprod* 70:846–859
- Chen W, Woodruff TK, Mayo KE 2000 Activin A-induced HepG2 liver cell apoptosis: involvement of activin receptors and smad proteins. *Endocrinology* 141:1263–1272
- Abdollah S, Macias-Silva M, Tsukazaki T, Hayashi H, Attisano L, Wrana JL 1997 T β RI phosphorylation of Smad2 on Ser465 and Ser467 is required for Smad2-Smad4 complex formation and signaling. *J Biol Chem* 272:27678–27685
- Souchelnytskyi S, Tamaki K, Engstrom U, Wernstedt C, ten Dijke P, Heldin CH 1997 Phosphorylation of Ser465 and Ser467 in the C terminus of Smad2 mediates interaction with Smad4 and is required for transforming growth factor- β signaling. *J Biol Chem* 272:28107–28115
- McMullen ML, Cho BN, Yates CJ, Mayo KE 2001 Gonadal pathologies in transgenic mice expressing the rat inhibin α -subunit. *Endocrinology* 142:5005–5014
- Resta L, Russo S, Colucci GA, Prat J 1993 Morphologic precursors of ovarian epithelial tumors. *Obstet Gynecol* 82:181–186
- Dietl J, Marzusch K 1993 Ovarian surface epithelium and human ovarian cancer. *Gynecol Obstet Invest* 35:129–135
- Jacobs I, Bast Jr RC 1989 The CA 125 tumour-associated antigen: a review of the literature. *Hum Reprod* 4:1–12
- Kabawat SE, Bast Jr RC, Bhan AK, Welch WR, Knapp RC, Colvin RB 1983 Tissue distribution of a coelomic-epithelium-related antigen recognized by the monoclonal antibody OC125. *Int J Gynecol Pathol* 2:275–285
- Dubeau L 1999 The cell of origin of ovarian epithelial tumors and the ovarian surface epithelium dogma: does the emperor have no clothes? *Gynecol Oncol* 72:437–442
- Hu X, Zuckerman KS 2001 Transforming growth factor: signal transduction pathways, cell cycle mediation, and effects on hematopoiesis. *J Hematother Stem Cell Res* 10:67–74
- Massague J 2000 How cells read TGF- β signals. *Nat Rev Mol Cell Biol* 1:169–178
- McCluggage WG, Weir PE 2000 Paraovarian cystic endosalpingiosis in association with tamoxifen therapy. *J Clin Pathol* 53:161–162
- Chodankar R, Kwang S, Sangiorgi F, Hong H, Yen HY, Deng C, Pike MC, Shuler CF, Maxson R, Dubeau L 2005 Cell-nonautonomous induction of ovarian and uterine serous cystadenomas in mice lacking a functional Brcal in ovarian granulosa cells. *Curr Biol* 15:561–565
- Jain T, Klein NA, Lee DM, Sluss PM, Soules MR 2003 Endocrine assessment of relative reproductive age in normal eumenorrheic younger and older women across multiple cycles. *Am J Obstet Gynecol* 189:1080–1084
- Santoro N, Isaac B, Neal-Perry G, Adel T, Weingart L, Nussbaum A, Thakur S, Jinnai H, Khosla N, Barad D 2003 Impaired folliculogenesis and ovulation in older reproductive aged women. *J Clin Endocrinol Metab* 88:5502–5509
- Elting MW, Kwee J, Korsen TJ, Rekers-Mombarg LT, Schoemaker J 2003 Aging women with polycystic ovary syndrome who achieve regular menstrual cycles have a smaller follicle cohort than those who continue to have irregular cycles. *Fertil Steril* 79:1154–1160
- Klein NA, Battaglia DE, Fujimoto VY, Davis GS, Bremner WJ, Soules MR 1996 Reproductive aging: accelerated ovarian follicular development associated with a monotropic follicle-stimulating hormone rise in normal older women. *J Clin Endocrinol Metab* 81:1038–1045
- Dahlgren E, Johansson S, Lindstedt G, Knutsson F, Oden A, Janson PO, Mattson LA, Crona N, Lundberg PA 1992 Women with polycystic ovary syndrome wedge resected in 1956 to 1965: a long-term follow-up focusing on natural history and circulating hormones. *Fertil Steril* 57:505–513
- Jefferson WN, Couse JF, Padilla-Banks E, Korach KS, Newbold RR 2002 Neonatal exposure to genistein induces estrogen receptor (ER) α expression and multiocyte follicles in the maturing mouse ovary: evidence for ER β -mediated and nonestrogenic actions. *Biol Reprod* 67:1285–1296